

## BATTERY ENERGY STORAGE SYSTEM (BESS) MODELING FOR MICROGRID

ZAHIR ZULKIFLY, SITI HAJAR YUSOFF\*, NOR LIZA TUMERAN  
AND NUR SYAZANA IZZATI RAZALI

*Department of Electrical and Computer Engineering, Kulliyah of Engineering,  
International Islamic University Malaysia, Jalan Gombak, 53100 Kuala Lumpur, Malaysia*

*\*Corresponding author: siti Yusoff@iium.edu.my*

*(Received: 12<sup>th</sup> May 2022; Accepted: 9<sup>th</sup> August 2022; Published on-line: 4<sup>th</sup> January 2023)*

**ABSTRACT:** In the age of technology, microgrids have become well known because of their capability to back up the grid when an unpleasant event is about to occur or during power disruptions, at any time. However, the microgrid will not function well during power disruptions if the controller does not respond fast enough and the BESS will be affected. Many types of controllers can be used for microgrid systems. The controllers may take the form of Maximum Power Point Tracking (MPPT) Controller, Proportional Integral Derivative (PID) Controller, and Model Predictive Controller (MPC). Each of the controllers stated has its functions for the microgrid. However, two controllers that must be considered are PID and MPC. Both controllers will be compared based on their efficiency results which can be obtained through simulations by observing both graphs in charging and discharging states. Most researchers implied that MPC is better than PID because of several factors such as MPC is more robust and stable because of its complexity. Other than that, MPC can handle more inputs and outputs than PID which can cater to one input and output only. Although MPC has many benefits over the PID, still it is not ideal due to its complex algorithm. This work proposed an algorithm of simulations for the MPC to operate to get the best output for microgrid and BESS and compare the performance of MPC with PID. Using Simulink and MATLAB as the main simulation software is a very ideal way to simulate the dynamic performance of MPC. Furthermore, with Simulink, unpredictable variables such as Renewable Energy (RE) sources input and loads demands that are related to MPC can be measured easily. The algorithm of MPC is a cost function. Then the performance of the MPC is calculated using Fast-Fourier Transform (FFT) and Total Harmonic Distortion (THD). Lower THD means a higher power factor, this results in higher efficiency. This paper recorded THD of 9.57% and 12.77% in charging states and 16.51% and 18.15% in discharging states of MPC. Besides, PID recorded THD of 22.10% and 29.73% in charging states and 84.29% and 85.58% in discharging states. All of the recorded THD is below 25% in MPC and it shows a good efficiency while PID's THD is above 25% shows its inefficiency.

**ABSTRAK:** Pada zaman teknologi, mikrogrid menjadi terkenal kerana keupayaannya untuk menjana kuasa grid apabila kejadian yang tidak menyenangkan bakal berlaku atau ketika terjadinya gangguan kuasa, pada bila-bila masa. Walau bagaimanapun, mikrogrid tidak dapat berfungsi dengan baik semasa gangguan kuasa jika alat kawalan tidak bertindak balas dengan cukup pantas dan BESS akan terjejas. Banyak alat kawalan (pengawal) boleh digunakan bagi keseluruhan sistem mikrogrid. Setiap pengawal adalah berbeza seperti Pengawal Penjejakan Titik Kuasa Maksimum (MPPT), Pengawal Berkadar Terbitan Kamilan (PID) dan Pengawal Model Ramalan (MPC). Setiap pengawal yang dinyatakan mempunyai fungsinya yang tersendiri bagi mikrogrid. Walau bagaimanapun, dua pengawal yang perlu dipertimbangkan adalah PID dan MPC. Kedua-dua pengawal ini akan dibandingkan berdasarkan keputusan kecekapan yang boleh

didapati melalui simulasi dengan memerhati kedua-dua graf pada keadaan pengecasan dan nyahcas. Ramai penyelidik menganggap bahawa MPC adalah lebih baik berbanding PID kerana beberapa faktor seperti MPC lebih teguh dan stabil kerana kerumitannya. Selain itu, MPC dapat mengendalikan lebih banyak input dan output berbanding PID yang hanya dapat menyediakan satu input dan output sahaja. Walaupun MPC mempunyai banyak faedah berbanding PID, ianya masih tidak sesuai kerana algoritma yang kompleks. Kajian ini mencadangkan algoritma simulasi bagi MPC beroperasi mendapatkan output terbaik untuk mikrogrid dan BESS dan membandingkan prestasi MPC dengan PID. Perisian simulasi utama yang sangat ideal bagi mensimulasi prestasi dinamik MPC adalah dengan menggunakan Simulink dan MATLAB. Tambahan, dengan Simulink, pembolehubah yang tidak terjangka seperti sumber Tenaga Boleh Diperbaharui (RE) dan permintaan beban yang berkaitan MPC boleh diukur dengan mudah. Algoritma MPC adalah satu fungsi kos. Kemudian prestasi MPC dikira menggunakan Penjelmaan Fourier Pantas (FFT) dan Total Pengherotan Harmonik (THD). THD yang lebih rendah bermakna faktor kuasa meningkat, ini menghasilkan kecekapan yang lebih tinggi. Kajian ini mencatatkan THD sebanyak 9.57% dan 12.77% dalam keadaan mengecas dan 16.51% dan 18.15% dalam keadaan nyahcas oleh MPC. Selain itu, PID mencatatkan THD sebanyak 22.10% dan 29.73% dalam keadaan mengecas dan 84.29% dan 85.58% dalam keadaan nyahcas. Semua THD yang direkodkan adalah di bawah 25% bagi MPC dan ia menunjukkan kecekapan yang baik manakala THD bagi PID adalah melebihi 25% menunjukkan ketidakcekapan.

---

**KEYWORDS:** *maximum power point tracker (MPPT) controller; proportional integral derivative (PID) controller; model predictive controller (MPC); battery energy storage system (BESS)*

## 1. INTRODUCTION

Today, many countries have been slowly exchanging the generation of electricity from non-renewable energy to renewable energy such as biomass, solar, and wind energy. In Malaysia, the government has announced to increase power generation using renewable resources to 20% from 2%. In [1], it stated that Malaysia has higher opportunities in solar power generation than other types of renewable energy. This is because Malaysia is located near the equator where the amount of sun irradiation is high [1]. The photovoltaic (PV) system is applied to harvest solar power.

The PV system is a power system that generates electricity directly from sunlight using PV cells. When sunlight strikes a PV cell's surface, it transforms light energy into electrical energy using the principle of forming a potential energy difference between photons and electrons. The combination of PV cells is called PV panel and the combination of PV panels is called PV module/array as can be seen in Fig. 1 [2], [3]. PV modules that are connected to the utility grid are called grid-connected PV (GCPV) systems. Other than that, a PV module that is not linked to the utility grid is called a stand-alone PV system. PV systems consist of several components to meet the goal of each system [4]. [3] said that GCPV and stand-alone PV have different components and configurations, thus both have different performances. GCPVs excess electricity generated from the solar module can be sold to the grid, hence it does not require a battery in the system. However, a stand-alone PV needs batteries to keep excess electricity generated by the solar panels, and this type of PV system is usually for the consumer that lives far from the city [3]. Figure 2 illustrates the types of PV systems in a hierarchy chart [4]. A single GCPV system usually consists of power conditioning units, inverters, solar panels, and grid connection equipment. Most GCPV systems are related to the microgrid.

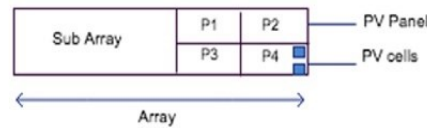


Fig. 1: The illustration of PV cell, PV panel, and PV array [3].

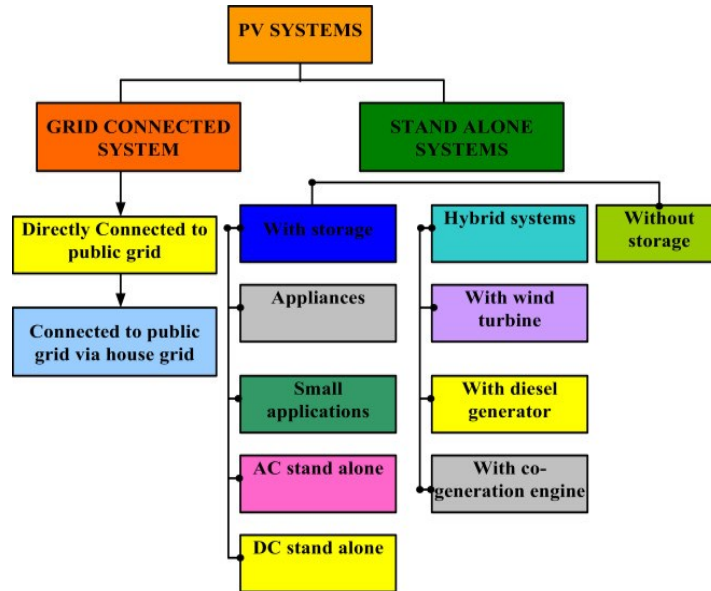


Fig. 2: The types of PV systems [4].

The microgrid is a type of electric power distribution system that consists of distributed energy resources (DER), interconnected loads, and various types of the consumer of electrical devices [5], [6]. Microgrids are not only able to supply small electrical devices but are also able to supply the full power needed by the consumer [7]. Moreover, the microgrid runs in a grid-connected mode through the subsidiary station transformer. When the grid is unable to operate, the microgrid will provide enough power to supply electricity to the end-user and remain operational as an autonomous (island-mode) entity [8]. However, for the microgrid to run smoothly, a high level of maintenance is needed. In this regard, a distributed energy storage system (ESS), distributed generation (DG) power, interlinking converter (IC), and controller are needed to develop system reliability [9]. A common microgrid structure including loads and distributed energy resource units is illustrated in Fig. 3 [10].

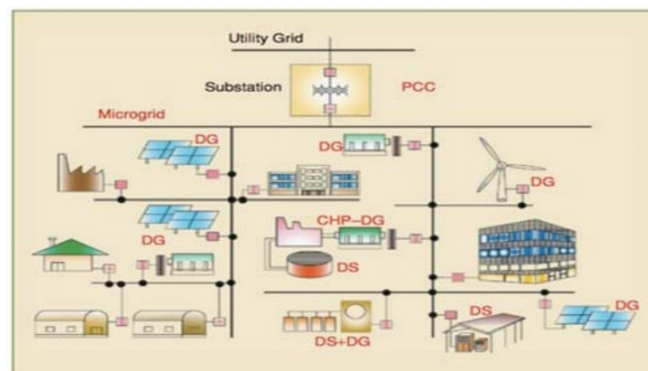


Fig. 3: Common microgrid structure integrating DERs and loads [10].

Nowadays, there are several common types of microgrids such as campus/institutional microgrids [11], military microgrids [12], and commercial and industrial microgrids [13] most of which have an architecture with AC-DC power systems or hybrid AC-DC microgrids [14] as shown in Fig. 4.

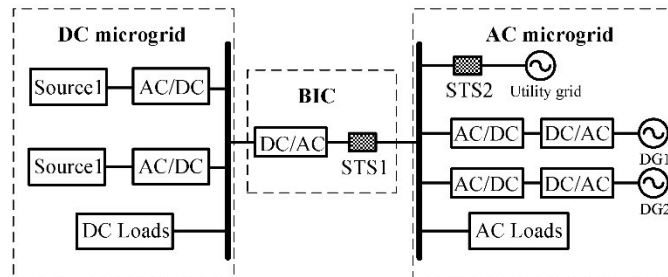


Fig. 4: Common microgrid structure integrating DERs and loads [14].

The hybrid microgrid is commercially used because of its efficiency that can easily change the architecture of the microgrid from islanded to grid-connected mode and reduce the conversion steps of AC power to DC power and vice versa [9]. Although it is a good power system, AC-DC architecture still has its drawback due to the interface power electronic converter [15]. This will disrupt the quality of power supply for both AC and DC networks.

The effect of the quality is majorly based on the controller and BESS. A microgrid controller is equipment that allows initializing of a microgrid by controlling DER and loads in an electrical system to maintain voltage and frequency in an optimized condition [16]. While BESS are rechargeable battery systems used for storing electric charges and providing them to homes or businesses. They are very efficient in handling difficult tasks, such as peak shaving and load shifting [17] and maintaining the reliability of the system (intake excess power generation or supply power to loads during power shortage) [18]. Both are important in the microgrid to maintain the quality of power which, if not handled properly, would create output power fluctuations [19], [20].

Several controllers are commonly used in microgrids such as the PID controller, the MPPT controller, and the MPC [21], [22]. However, the most used controller is the MPC. [23] states that the MPC has a better performance than the PID in terms of vehicle control and the enhanced MPC has the fastest response in the drone's movement control [24]. Besides, [25] remarks that the MPC is more robust and stable because of its complexity. Paper [26] explains that the MPC can handle more inputs whereas the PID can only cater to one input and output. MPC is a control technology that makes use of past information and model prediction to predict the process output which is the characteristic of a system's arbitrary number of sampling steps into a timeline view based on a set of the reference control signal and predicted variable [27], [28]. According to Panda and Arnab's [18] research, MPC is used to control the AC grid side inverters and DC grid side converters. This approach is to enhance the power quality and reliability of the grid. Other than that, MPC is used to improve cost optimization, single-period horizon prediction, and monitoring output voltage. Furthermore, the use of MPC has been increasing in the microgrid where it acts as the controller. MPC has also been applied to many other industrial-related applications due to its efficiency [28-30]. The reason why MPC is preferable to be implemented in a microgrid is that the microgrid depends on RES (solar and wind energy) and BESS which cause uncertainties in load demand during the day, night, and unpleasant weather [31]. Babayomi et al. [32] expressed that the MPC can cope

with complex and dynamic systems with multiple inputs and outputs and systems with uncertainties and disturbances and even reduce the computational operation [33]. The microgrid is therefore an optimal control strategy [27], as shown in Fig. 5.

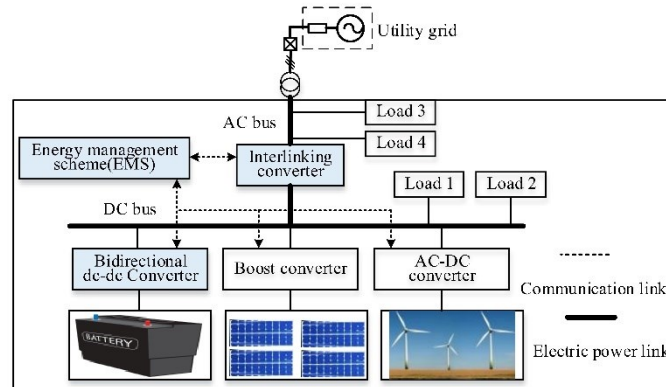


Fig. 5: Microgrid with multiple energy sources and converters [27].

Based on the figure described by Shan et al. [27], there are two parts critically involved: the AC sub-grid with AC loads and the DC sub-grid with DC loads. The AC and DC buses are connected to each other via bidirectional AC-DC IC. In this system, predictive voltage and power (MPVP) and model predictive current and power (MPCP) control models are both utilized. While MPVP is used to regulate the AC-DC IC., MPCP is employed to manage the bidirectional DC-DC converter in BESS. A DC-DC converter connects BESS to the DC bus. Both controls are applied to regulate the DC-DC converter and the AC-DC converter for reliable DC and AC bus voltage and smooth RE outputs.

Other than that, BESS, with good performance while charging and discharging, is needed for microgrid control. Yilmaz et al. [29] stated that the overall performance of BESS is solely dependent on control performance, MPC, which needs a predictive variable. With the aid of MPC, BESS's role in a microgrid is to make up for forecasting errors and lower operating costs brought on by RES and load demand. Additionally, MPC controls the power consumed or supplied by BESS, which is necessary to obtain the predictive variables. To maintain the power balance within microgrids, the BESS should discharge and charge accordingly [27].

In this paper, the simulation of MPC in a microgrid with BESS is done in MATLAB/SIMULINK. A model in the MATLAB/SIMULINK is made and the performance of MPC is tested using Fast-Fourier Transform (FFT).

## 2. ANALYSIS OF MICROGRID COMPONENT

Concerning BESS, one aspect that must be compliant before using it in any system is the state of charge (SoC). SoC is the proportion of a battery's nominal capacity to its capacity at a time. SoC detects the battery capacity, 100% denotes a full charge, while 0% denotes an empty battery [34]. Mu and Xiong [35] give the equation for the SoC ratio, as shown in Eq. (1):

$$SoC_t = SoC_0 - \int_0^t \eta_i I_L \tau d\tau / C_a \quad (1)$$

where

$SoC_t$  = present SoC



SoC<sub>0</sub> = SoC initial value

I<sub>L</sub> = instantaneous load current

n<sub>i</sub> = Coulomb efficiency

C<sub>a</sub> = present maximum available capacity

The output of a PV generator is solely dependent on solar irradiance. If the weather is unpredictable with cloudy or rainy conditions, the PV output will surely fluctuate. Qian et al. [36] stated that, the result of the fluctuation will affect the power quality of the PV generator that is connected to BESS. The quality of the PV can be evaluated by the equation of Performance Ratio (PR) as informed in IEC 61724 as “Photovoltaic system performance monitoring: guidelines for measurement, data exchange, and analysis” [37]. The equation for PR is shown in Eq. (2):

$$PR = \frac{E_{AC}}{P_{MPP,NOM}^* \frac{G_{\Delta T}}{G^*}} \quad (2)$$

where

PR = Performance Ratio

E<sub>AC</sub> = energy sent to the grid efficiently

P<sub>MPP,NOM</sub><sup>\*</sup> = the product of the nameplate Standard Test Condition (STC) power and the quantity of PV modules in the system.

G<sub>ΔT</sub> = annual in-plane irradiation in a certain period

G<sup>\*</sup> = in-plane effective irradiance

Noted that STC is also known as rated power PV generator.

In the meantime, managing SoC is very important for BESS effectiveness and BESS sizing capacity. Other than that, controlling SoC can reduce the violation of the BESS’s SoC operating range during renewable integration continuously. SoC management of BESS is very important whenever PV and BESS are increasing rapidly. Other than that, the BESS that is connected to MPC needs predictive variables. The predictive variables of BESSs are set on the discrete-time model of converters.

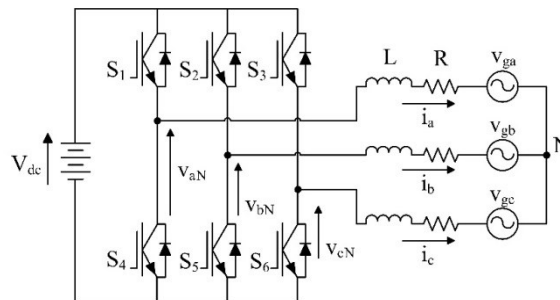


Fig. 6: Configuration of BESS.

From Fig. 6, [38] provided three equations that characterized the voltage V<sub>g</sub> of a three-phase AC power supply, using filter inductance L and resistance R.

$$V_{aN} = L \frac{di_a}{dt} + Ri_a + V_{ga} \quad (3)$$

$$V_{bN} = L \frac{di_b}{dt} + Ri_b + V_{gb} \quad (4)$$

$$V_{cN} = L \frac{di_c}{dt} + Ri_c + V_{gc} \quad (5)$$

Table 1: Switching states and voltage vectors

$x$	$S_a$	$S_b$	$S_c$	<i>Voltage Vectors, v</i>
1	0	0	0	$v_0 = 0$
2	1	0	0	$v_1 = \frac{2}{3}V_{dc}$
3	1	1	0	$v_2 = \frac{1}{3}V_{dc} + j\frac{\sqrt{3}}{3}V_{dc}$
4	0	1	0	$v_3 = -\frac{1}{3}V_{dc} + j\frac{\sqrt{3}}{3}V_{dc}$
5	0	1	1	$v_4 = -\frac{2}{3}V_{dc}$
6	0	0	1	$v_5 = -\frac{1}{3}V_{dc} - j\frac{\sqrt{3}}{3}V_{dc}$
7	0	1	1	$v_6 = \frac{1}{3}V_{dc} - j\frac{\sqrt{3}}{3}V_{dc}$
8	1	1	1	$v_7 = 0$

$$s(t) = \begin{cases} 1, & \text{discharge mode} \\ 0, & \text{charging mode} \end{cases} \quad (6)$$

$$i^p(k+1) = \left(1 - \frac{RT_s}{L}\right)I(k) + \frac{T_s}{L}(v(k) - v_g(k)) \quad (7)$$

$$P^p(k+1) = 1.5\text{Re}\{i^{-p}(k+1)v_g^m(k)\} \quad (8)$$

$$Q^p(k+1) = 1.5\text{Im}\{i^{-p}(k+1)v_g^m(k)\} \quad (9)$$

The derivation of Eq. (3) to Eq. (5) through space vector, switching states and voltage vectors (Table1) will give Eq. (6) which is the future current at the sampling instant  $k+1$ . From Eq. (6),  $i(k)$  and  $v_g(k)$  are the three-phase currents, and voltage of BESS measured at sampling instant  $k$  with sampling time  $T_s$ . They [38] also assumed that the voltage at sampling instant  $k+1$  equals to measured grid voltage at  $k$ th sampling instant ( $v_g(k+1) = v_g(k)$ ). As a result, the predicted instantaneous real and predictive powers are Eq. (7) and Eq. (8). Eq. (6) to Eq. (8) show that the predictive current and power rely on the system model, converter, and filter parameters. In the conclusion, inaccuracy in predictive variables will occur if there are any changes in the model parameters.

Furthermore, according to Fig. 7, there are two states of BESS, which are charging and discharging. The illustration proposed by Shan et al. [27] demonstrates the current flow between BESS, RES and the rest of the microgrid (ROM).

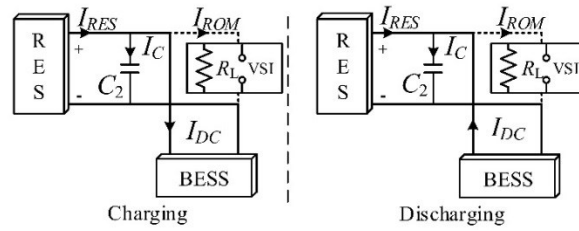


Fig. 7: Illustration of 2 states within the BESS system [27].

In order to charge or discharge the BESS, the cost function should be considered. So, they [27] proposed a cost function Eq. (9) to optimize BESS current.

$$J_c = |I_B^* - I_B(K + 1)| \quad (10)$$

$$s. t SOC_{min} \leq SOC \leq SOC_{max}, I_B \leq |I_{B\_rated}|$$

$$i_L^* * I_B^* \frac{(v_{dc}^*)^2}{R * v_b(k)} \quad (11)$$

- $I_B$  = Battery current.
- $I_B^*$  = Battery current set with electricity price in grid-connected operation.

From Fig. 7, the relationship between the currents can be obtained using Kirchoff's current law (KCL) in the form of an equation.

$$I_{DC} = I_{RES} - I_C - I_{ROM} \quad (12)$$

- $I_{DC}$  = current supplied/used by BESS.
- $I_{RES}$  = current from RES.
- $I_C$  = current flow of DC side capacitor.
- $I_{ROM}$  = current flow into DC loads and inverter.

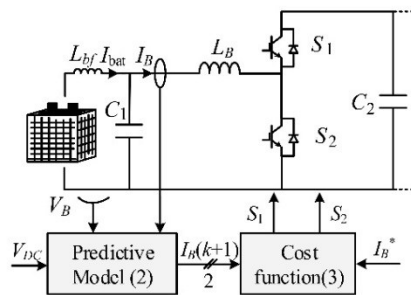


Fig. 8: Operation of BESS system in grid-connected microgrid [27].

In the meantime, proposed Fig. 8 by [27], showed the block diagram of the MPC strategy. They [27] said that, to control the charging and discharging current of BESS, the voltage  $V_B$ , current  $I_B$  and DC voltage  $V_{DC}$  are needed to predict the battery current  $I_B(k+1)$ .

A simple but effective MPC strategy for the Bidirectional converter is proposed, to improve its dynamic performance. The advantage of the presented strategy is that the problem is formulated in a way that only a one-step prediction horizon is needed to control



the converter. Therefore, a proper cost function elaborated in terms of the inductor current is proposed. The MPC working principle applied to the Bidirectional converter under study is illustrated in Fig. 9. Tables 2 to 4 listed the required parameters for the simulations of model predictive control in Simulink.

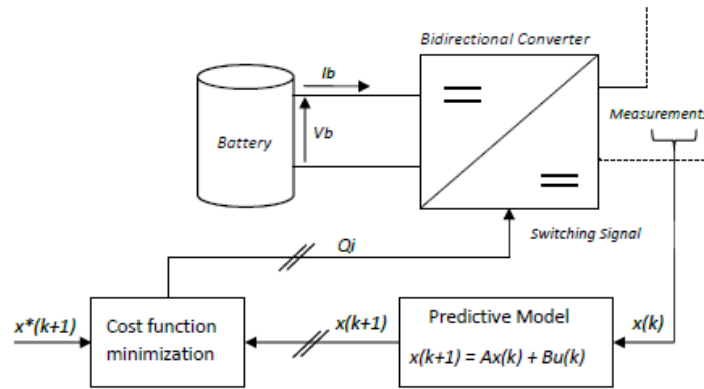


Fig. 9: Model Predictive Controller block diagram.

Table 2: Generic battery model parameters

Parameters	Formula	Value
Constant Battery Current, $I_b$		1.3 A
Rated Battery Capacity, $Q_o$		6.5 Ah
Internal Resistance, $R_b$		2 mΩ
Fully Charged Voltage, $V_{full}$		1.39 V
Exponential Voltage, $V_{exp}$		1.28 V
Nominal Voltage, $V_{nom}$		1.18 V
Exponential Capacity, $Q_{exp}$	$Q_{exp} = I_b * 1$	1.3 A
Nominal Capacity, $Q_{nom}$		6.25 Ah
Exponential Zone Amplitude, $A$	$A = V_{full} - V_{exp}$	0.11
Exponential Zone Time Constant Inverse, $B$	$B = 3/Q_{exp}$	2.3077
Polarization Voltage, $K$	$K = (V_{full} - V_{nom} + A * (exp(-B * Q_{nom}) - 1)) * (Q_o - Q_{nom}) / Q_{nom}$	0.004
Battery Constant Voltage, $E_o$	$E_o = V_{full} + K + R_b * I_b - A$	1.28

Table 3: Boost Converter Model parameters

Parameters	Value
PV Nominal Temperature	25°C
Irradiance	0 & 1000kW/m <sup>2</sup>
Power GUI	Discrete
PV Capacitance, $C_{PV}$	100 μF
PV Inductance, $L_{PV}$	5mH
Boost Capacitance, $C_{Boost}$	3300 μF
Load	5Ω

Table 4: Bidirectional Converter Model parameters

Parameters	Formula	Value
------------	---------	-------

Battery Type		Nickel-Metal-Hydride (NiMH)
Battery Capacitance, $C_{\text{Battery}}$ , $C_b$		700 $\mu$ F
Battery Inductance, $L_{\text{Battery}}$ , $L_b$		33mH
Output Capacitance, $C_2$		2mF
Load, $R$		5 $\Omega$
Measured Disturbance Signal, $v_b$		6V
Steady State Duty Cycle, $S$		0.5
Steady State DC Bus Voltage, $v_{dc}$	$v_b/(1-S)$	12V
Steady State Inductor Current, $i_L$	$v_{dc}/((1-S) * R)$	4.8A
DC Reference Voltage, $v_{dcref}$	$v_b/(1-S)$	12V

### 3. RESULT AND DISCUSSION

The proposed MPC strategy was implemented in the MATLAB programming interface, together with the battery and the bidirectional models, to simulate the performance of the control unit. The bidirectional model is a model that flows in two directions, forward and backward, thus connecting the battery with the bidirectional converter. Figure 10 shows the microgrid model with MPC control in Simulink.

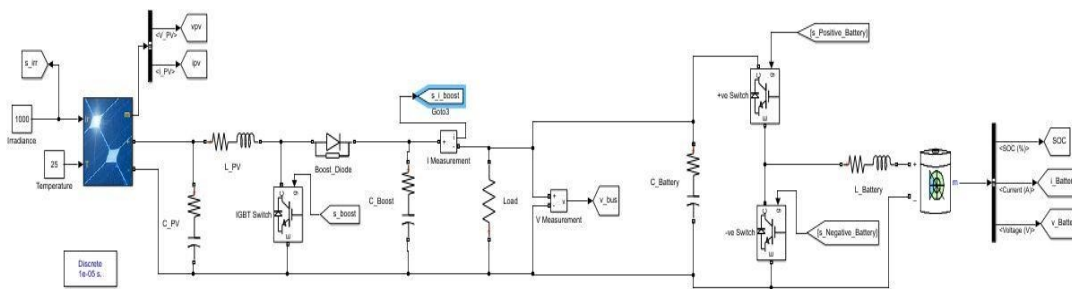


Fig. 10: The microgrid model with MPC in Simulink.

The simulation results for a start-up are shown in Fig. 9, using parameters given in Table 2 - 4. The purpose of the simulation is to simulate the performance of the control unit and optimize it by predicting the future behavior of controlled variables using MPC. However, the main purpose of using MPC is to reimburse the power difference between load and PV generation, during constant DC bus voltage [27].

Two states have been simulated, which are the charging state of battery and discharging state of battery. In Fig. 9, the output voltage ( $v_{dc}$ ) reaches its reference value in about 50 ms, the battery current ( $i_L$ ) is negative and below its nominal current and the DC bus voltage is constant at 6V ( $v_b$ ). This result is dependent and interconnected with Fig. 9, which shows the PV power generation is higher than the load demand while the battery is charged from it.

However, in Fig. 11, the results show the battery current is reaching its nominal current, while the output voltage results remain the same. For this scenario, it is shown that the load is powered by the battery, because in Fig. 14, the result shows the SoC of the battery is decreasing.

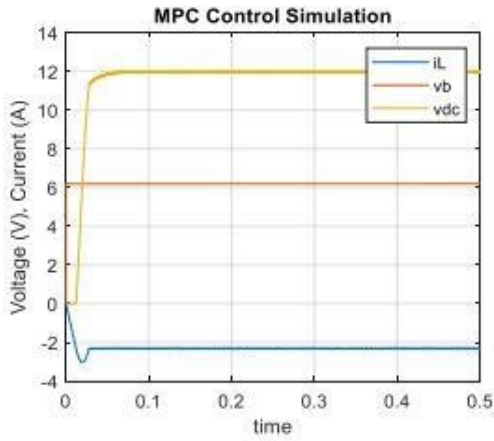


Fig. 11: MPC Control Simulation Results for Charging State.

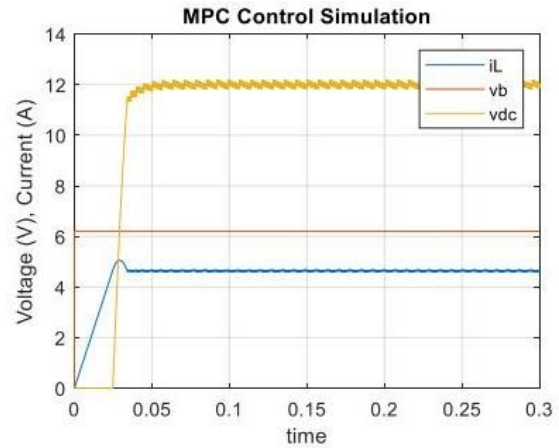


Fig. 12: MPC Control Simulation Results for Discharging State.

The performance of the suggested power management can be verified through simulation carried out using MATLAB programming interface based on Table 2 parameters. However, in this simulation, only charging and discharging will be considered as they are common situations for microgrids. Charging refers to daytime activity when the irradiance is high ( $1000 \text{ kW/m}^2$ ) while discharging refers to night-time activity when there is no irradiance ( $0 \text{ kW/m}^2$ ). The following figures illustrate the charging and discharging of the battery for different cases.

Figure 13 illustrates the charging state where there is excess power produced by the PV panel while the battery is not fully charged. This causes the power produced to charge the battery. For this case, SOC of the battery is initially at 60%, which then charges until 100% if there is irradiance for the time period. When the battery is fully charged, the MPPT controller will alert the PV to stop receiving power to avoid overcharge.

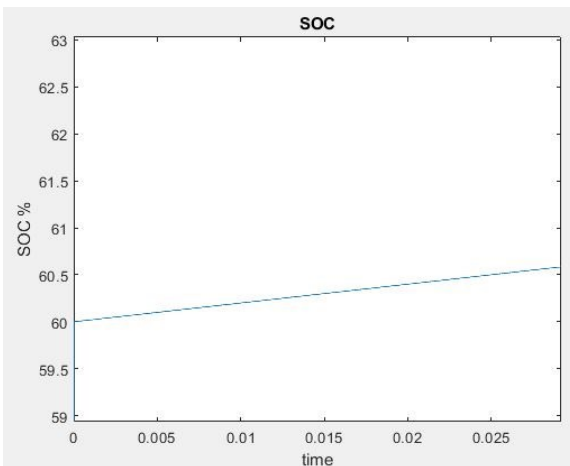


Fig. 13: MPC SOC Simulation Results for Charging State.

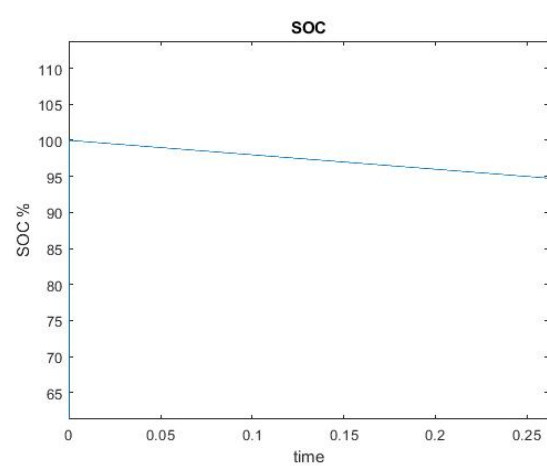


Fig. 14: MPC SOC Simulation Results for Discharging State.

Figure 14 illustrates the discharging state where there is no power produced from the PV panel and the load demand is supplied by the battery. For this case, the SOC of the battery is at 100% (fully charged) and it will continue to decrease until the load demand is supplied from the PV system.

The performance of the MPC can be shown and calculated by using FFT analysis. FFT analysis measures power supply or generator's output quality. The analysis aims to make sure the value of THD is maintained as low as possible. Lower THD means a higher power factor, which results in higher efficiency [39]. The acceptable THD value for generators is below 25%, while the best THD value for generators is below 10%.

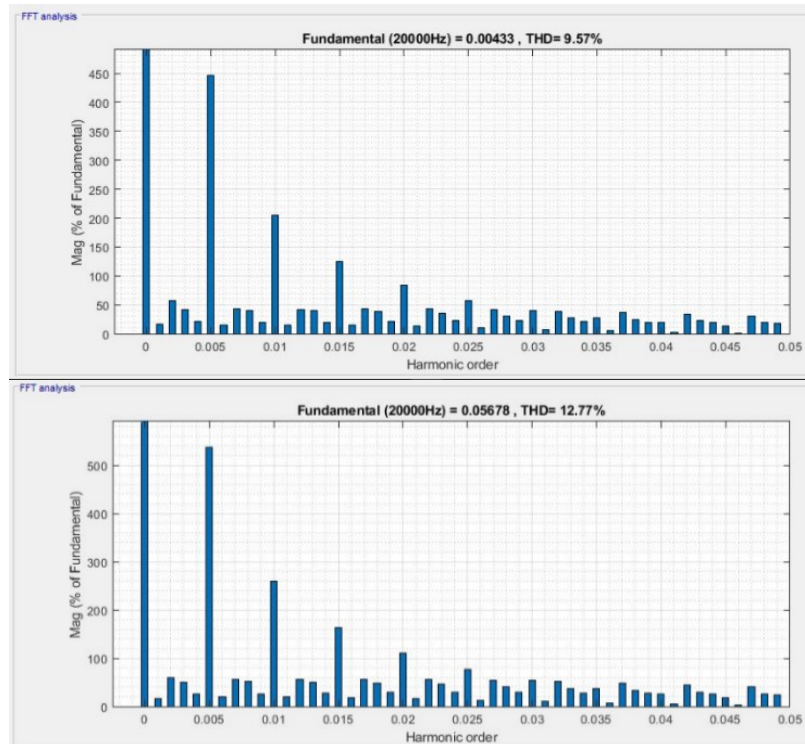


Fig. 15: MPC Charging voltage (above) and current (below) for FFT analysis.

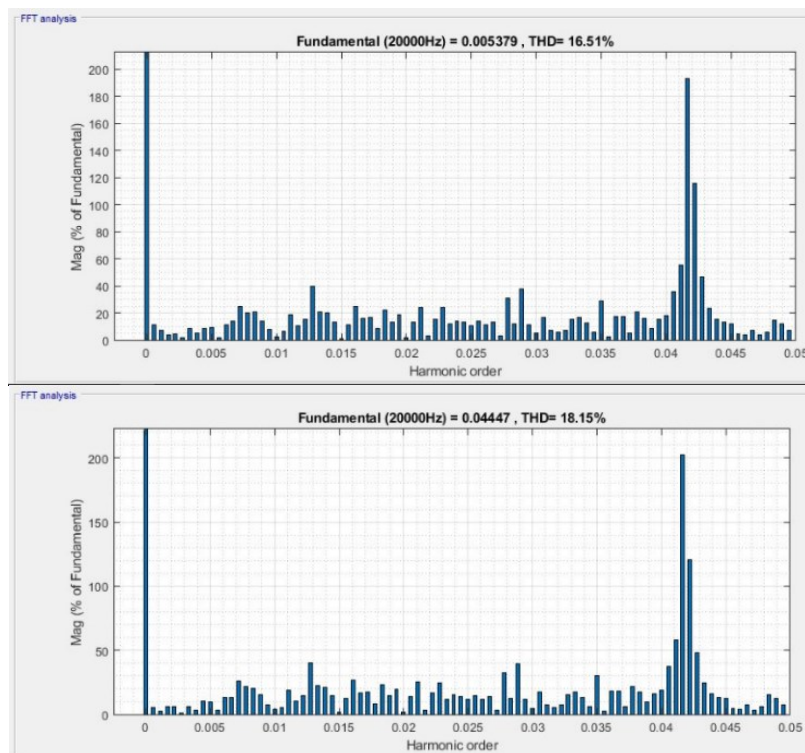


Fig. 16: MPC Discharging voltage (above) and current (below) for FFT analysis.

Based on Table 5 and according to [24], the THD value for both states are considered acceptable which is below 25% for the MPC. This proves that the generators are working efficiently when in a 20 kHz sampling rate.

Table 5: THD Value for Charging and Discharging States

Charging State	Output State	THD (MPC)
Charging	Voltage Output	9.57%
Charging	Current Output	12.77%
Discharging	Voltage Output	16.51%
Discharging	Current Output	18.15%

To compare the efficiency of MPC and PID, the simulation using PID has been done. Figures 17 and 18 show the charging and discharging voltage and current for FFT analysis. Table 6 compares the THD of MPC and PID. All of MPC's THD are acceptable, however, PID control is only stable when the control system is operating in charging state whereas in discharging state, the THD value is not acceptable and is above 25%. Thus, it can be seen that MPC is better in performance than PID.

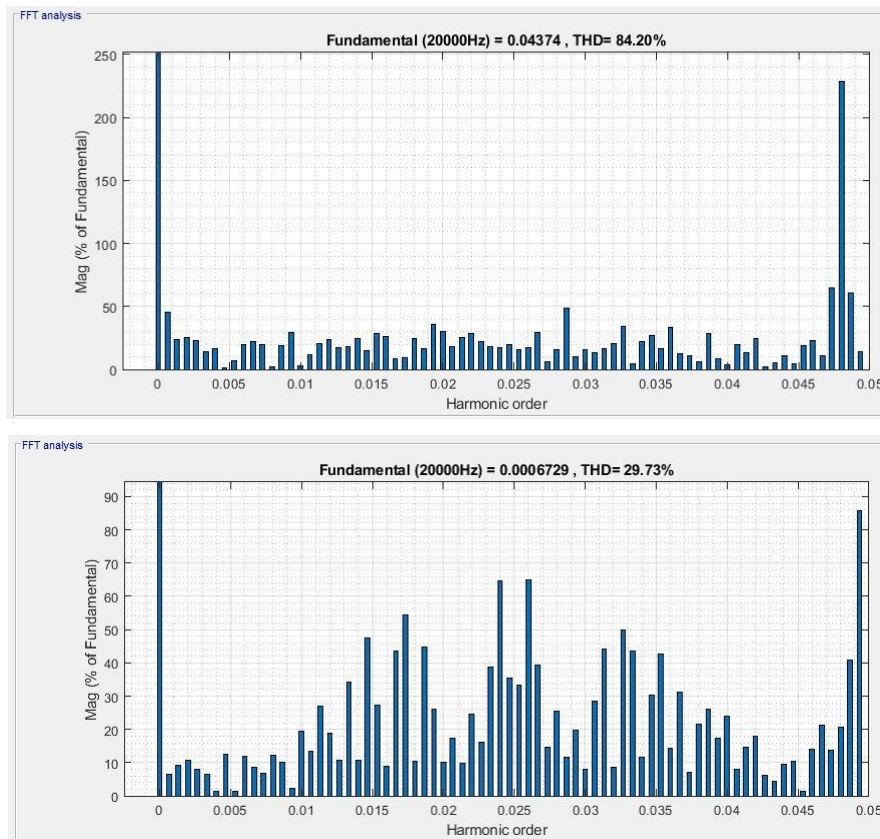


Fig. 17: PID Charging voltage (above) and current (below) for FFT analysis.



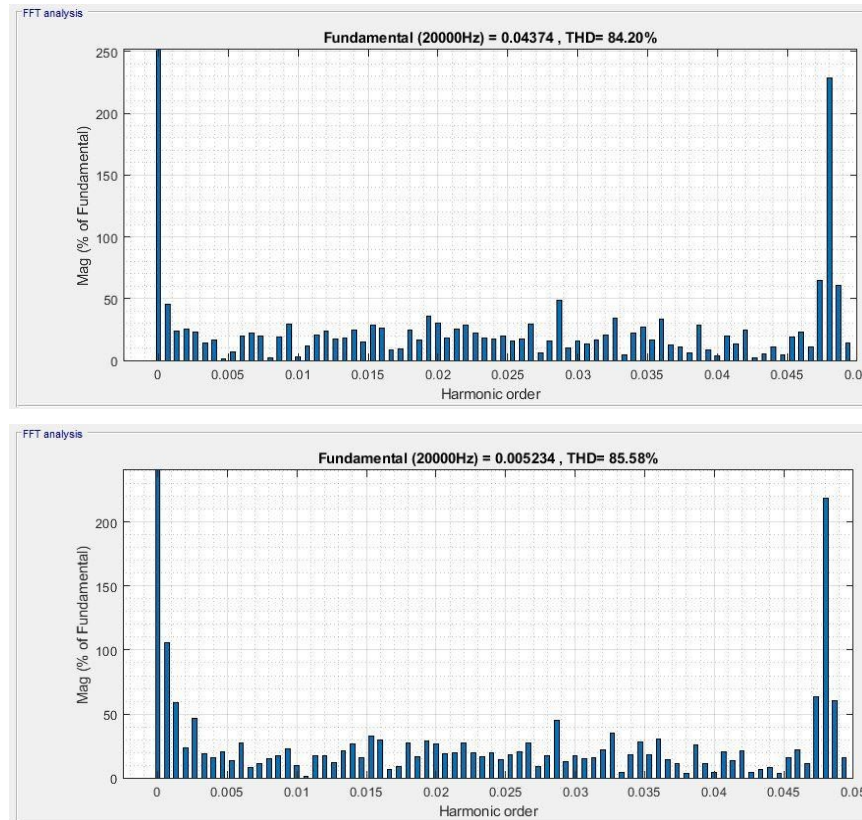


Fig. 18: PID Discharging voltage (above) and current (below) for FFT Analysis.

Table 6: THD Value for Charging and Discharging States

Charging State	Output State	THD (MPC)	THD (PID)
Charging	Voltage Output	9.57%	22.10%
Charging	Current Output	12.77%	29.73%
Discharging	Voltage Output	16.51%	84.29%
Discharging	Current Output	18.15%	85.58%

#### 4. CONCLUSION

Microgrids have been used for many purposes every day. A microgrid is a self-sufficient energy system that consist of distributed generating units, loads, and control units. By using microgrids, one can save costs and reduce global warming. However, microgrids are not as simple as they seem. One of the basic elements of microgrids is its brain, aka its control unit(s). The control unit controls all the actions between the distributed generator and loads. Earlier, engineers used PID control as the control unit. However, PID control is not efficient in the case of unpredicted events that cause instantaneous disturbance to the microgrid. Later, when MPCs were introduced, they replaced all the PID control making MPCs the new brains in microgrids. MPCs gained favor because their algorithm can predict various outputs in the future with multiple inputs. This paper proposed an algorithm for the MPC using cost functions. To prove MPCs efficiency, this paper proposed to compare it with PID control. At the end of the experiment, it can be concluded that the MPC is better than PID control in terms of efficiency. In future work, other types of battery such as Li-ion and Li-Po, should be used. The battery type that was used in this simulation is nickel-metal hydride (Ni-MH) and its



performance is not affected by changes in temperature. However, to get better MPC performance, batteries such as Li-ion and Li-Po are needed because the temperature will affect the performance of these batteries.

## ACKNOWLEDGEMENT

This work was partially supported under IIUM-UMP-UITM Sustainable Research Collaboration Grant 2020 (SRCG) number SRCG20-049-0049.

## REFERENCES

- [1] Abdullah WSW, Osman M, Kadir MZAA, Verayiah R. (2019). The Potential and Status of Renewable Energy Development in Malaysia. *Energies*, 12: 2437. <https://doi.org/10.3390/EN12122437>
- [2] Rakesh Tej Kumar K, Ramakrishna M, Durga Sukumar G. (2018). A review on PV cells and nanocomposite-coated PV systems. *International Journal of Energy Research*, 42(7): 2305-2319. <https://doi.org/10.1002/ER.4002>
- [3] Usman Z, Tah J, Abanda H, Nche C. (2020). A Critical Appraisal of PV-Systems' Performance. *Buildings*, 10: 192. <https://doi.org/10.3390/BUILDINGS10110192>
- [4] Koondhar MA, Laghari IA, Asfaw BM, Reji Kumar R, Lenin AH. (2022). Experimental and simulation-based comparative analysis of different parameters of PV module. *Scientific African*, 16: e01197. <https://doi.org/10.1016/J.SCIAF.2022.E01197>
- [5] Kumar J, Agarwal A, Singh N. (2020). Design, operation and control of a vast DC microgrid for integration of renewable energy sources. *Renewable Energy Focus*, 34: 17-36. <https://doi.org/10.1016/j.ref.2020.05.001>
- [6] Badruhisam SH, Shahrin M, Hanifah A, Yusoff S H, Hasbullah NF, Yaacob M. (2021). Integration of Hybrid Biomass-Solar Photovoltaic- Wind turbine in Microgrid Application. 2021 8th International Conference on Computer and Communication Engineering (ICCCCE), 87-92.
- [7] Hirsch A, Parag Y, Guerrero J (2018). Microgrids: A review of technologies, key drivers, and outstanding issues. *Renewable and Sustainable Energy Reviews*, 90: 402-411. <https://doi.org/10.1016/j.rser.2018.03.040>
- [8] Wu T, Ye F, Su Y, Wang Y, Riffat S. (2019). Coordinated control strategy of DC microgrid with hybrid energy storage system to smooth power output fluctuation. *International Journal of Low-Carbon Technologies*, 15: 46-54. <https://doi.org/10.1093/ijlct/ctz056>
- [9] Ahmed M, Meegahapola L, Vahidnia A, Datta M. (2020). Stability and Control Aspects of Microgrid Architectures-A Comprehensive Review. *IEEE Access*, 8:144730-144766. <https://doi.org/10.1109/ACCESS.2020.3014977>
- [10] Alhamrouni I, Hairullah MA, Omar NS, Salem M, Jusoh A, Sutikno T. (2019). Modelling and design of PID controller for voltage control of AC hybrid micro-grid. *International Journal of Power Electronics and Drive Systems*, 10: 151-159. <https://doi.org/10.11591/ijpeds.v10n1.pp151-159>
- [11] Shahgholian G. (2021). A brief review on microgrids: Operation, applications, modeling, and control. <https://doi.org/10.1002/2050-7038.12885>
- [12] Barry NG, Santoso S. (2021). Military Diesel Microgrids: Design, Operational Challenges, Energy Storage Integration. *IEEE Power and Energy Society General Meeting*, 2021-July. <https://doi.org/10.1109/PESGM46819.2021.9637999>
- [13] Guarnieri M, Bovo A, Giovannelli A, Mattavelli P. (2018). A Real Multitechnology Microgrid in Venice: A Design Review. *IEEE Industrial Electronics Magazine*, 12(3) :19-31. <https://doi.org/10.1109/MIE.2018.2855735>
- [14] Jiao J, Meng R, Guan Z, Ren C, Wang L, Zhang B. (2019). Grid-connected control strategy for bidirectional AC-DC interlinking converter in AC-DC hybrid microgrid.

- PEDG 2019 - 2019 IEEE 10th International Symposium on Power Electronics for Distributed Generation Systems. <https://doi.org/10.1109/PEDG.2019.8807601>
- [15] Wei B, Han X, Wang P, Yu H, Li W, Guo L (2020). Temporally coordinated energy management for AC/DC hybrid microgrid considering dynamic conversion efficiency of bidirectional AC/DC converter. *IEEE Access*, 8: 70878–70889. <https://doi.org/10.1109/ACCESS.2020.2985419>
- [16] Newaz S, Naiem-Ur-Rahman M (2020). Voltage Control of Single Phase Islanded Microgrid by Fuzzy Logic Controller for Different Loads. 2020 IEEE Region 10 Symposium, TENSYP 2020, June, 1560-1563. <https://doi.org/10.1109/TENSYP50017.2020.9230686>
- [17] Alshehri J, Khalid M (2019). Power quality improvement in microgrids under critical disturbances using an intelligent decoupled control strategy based on battery energy storage system. *IEEE Access*, 7: 147314-147326. <https://doi.org/10.1109/ACCESS.2019.2946265>
- [18] Kumar Panda S, Ghosh A. (n.d.). A Computational Analysis of Interfacing Converters with Advanced Control Methodologies for Microgrid Application. <https://doi.org/10.1007/s40866-020-0077-x>
- [19] Chen X, Shi M, Zhou J, Chen Y, Zuo W, Wen J, He H. (2020). Distributed Cooperative Control of Multiple Hybrid Energy Storage Systems in a DC Microgrid Using Consensus Protocol. *IEEE Transactions on Industrial Electronics*, 67(3): 1968-1979. <https://doi.org/10.1109/TIE.2019.2898606>
- [20] Hu J, Shan Y, Xu Y, Guerrero JM. (2019). A coordinated control of hybrid ac/dc microgrids with PV-wind-battery under variable generation and load conditions. *International Journal of Electrical Power and Energy Systems*, 104: 583-592. <https://doi.org/10.1016/j.ijepes.2018.07.037>
- [21] Sarkar SK, Badal FR, Das SK. (2018). A comparative study of high performance robust PID controller for grid voltage control of islanded microgrid. *International Journal of Dynamics and Control*, 6(3):1207-1217. <https://doi.org/10.1007/s40435-017-0364-0>
- [22] Sarkar SK, Badal FR, Das SK, Miao Y. (2018). Discrete time model predictive controller design for voltage control of an islanded microgrid. 3rd International Conference on Electrical Information and Communication Technology, EICT 2017, 2018-Janua (December), 1-6. <https://doi.org/10.1109/EICT.2017.8275162>
- [23] Varma B, Swamy N, Mukherjee S. (2020). Trajectory Tracking of Autonomous Vehicles using Different Control Techniques (PID vs LQR vs MPC). *Proceedings of the International Conference on Smart Technologies in Computing, Electrical and Electronics, ICSTCEE 2020*, 84-89. <https://doi.org/10.1109/ICSTCEE49637.2020.9276986>
- [24] Okulski M, Ławryńczuk M. (2022). How Much Energy Do We Need to Fly with Greater Agility? Energy Consumption and Performance of an Attitude Stabilization Controller in a Quadcopter Drone: A Modified MPC vs. PID. *Energies*, 15(4): 1380. <https://doi.org/10.3390/EN15041380>
- [25] Haber R, Rossiter JA, Zabet K. (2016). An alternative for PID control: Predictive Functional Control - A tutorial. *Proceedings of the American Control Conference*, 2016-July, 6935-6940. <https://doi.org/10.1109/ACC.2016.7526765>
- [26] Kozák Š. (2016). From PID to MPC: Control engineering methods development and applications. 2016 Cybernetics and Informatics, K and I 2016 - Proceedings of the 28th International Conference. <https://doi.org/10.1109/CYBERI.2016.7438634>
- [27] Shan Y, Hu J, Chan KW, Fu Q, Guerrero JM (2019). Model Predictive Control of Bidirectional DC-DC Converters and AC/DC Interlinking Converters-A New Control Method for PV-Wind-Battery Microgrids. *IEEE Transactions on Sustainable Energy*, 10(4):1823-1833. <https://doi.org/10.1109/TSTE.2018.2873390>
- [28] Chen M, Xu Z, Zhao J (2020). Triple-mode model predictive control using future target information. *Processes*, 8(1), 54. <https://doi.org/10.3390/pr8010054>
- [29] Can Yilmaz U, Erdem Sezgin M, Gol M (n.d.). A Model Predictive Control for Microgrids Considering Battery Aging. <https://doi.org/10.35833/MPCE.2018.000804>.

- [30] Yusoff SH, Midi NS, Khan S, Tohtayong M. (2017). Predictive control of AC/AC matrix converter. *International Journal of Power Electronics and Drive Systems*, 8(4): 1932-1942. <https://doi.org/10.11591/ijpeds.v8i4.pp1932-1942>
- [31] Abbasi M, Dehkordi NM, Sadati N. (2020). Decentralized Model Predictive Voltage Control of Islanded DC Microgrids. 2020 11th Power Electronics, Drive Systems, and Technologies Conference, PEDSTC 2020. <https://doi.org/10.1109/PEDSTC49159.2020.9088498>
- [32] Babayomi O, Li Y, Zhang Z, Kennel R, Kang J. (2020). Overview of Model Predictive Control of Converters for Islanded AC Microgrids. 2020 IEEE 9th International Power Electronics and Motion Control Conference, IPEMC 2020 ECCE Asia, 1023-1028. <https://doi.org/10.1109/IPEMC-ECCEAsia48364.2020.9368069>
- [33] Lee J, Chang HJ. (2018). Analysis of explicit model predictive control for path-following control. *PLoS ONE*, 13(3):1-19. <https://doi.org/10.1371/journal.pone.0194110>
- [34] Zahid T, Xu K, Li W, Li C, Li H. (2018). State of charge estimation for electric vehicle power battery using advanced machine learning algorithm under diversified drive cycles. *Energy*, 162:871–882. <https://doi.org/10.1016/J.ENERGY.2018.08.071>
- [35] Yao C, Ruan X, Wang X. (2010). Isolated buck-boost DC/DC converter for PV grid-connected system. *IEEE International Symposium on Industrial Electronics*, 889-894. <https://doi.org/10.1109/ISIE.2010.5637196>
- [36] Long Q, Yu H, Xie F, Zeng W, Lukic S, Lu N, Lubkeman D. (2020). Microgrid power flow control with integrated battery management functions. *IEEE Power and Energy Society General Meeting*, August. <https://doi.org/10.1109/PESGM41954.2020.9281437>
- [37] de la Parra I, Muñoz M, Lorenzo E, García M, Marcos J, Martínez-Moreno F. (2017). PV performance modelling: A review in the light of quality assurance for large PV plants. *Renewable and Sustainable Energy Reviews*, 78: 780-797. <https://doi.org/10.1016/J.RSER.2017.04.080>
- [38] Nguyen T-T, Yoo H-J, Kim H-M. (2015). Application of Model Predictive Control to BESS for Microgrid Control. 8:8798-8813. <https://doi.org/10.3390/en8088798>
- [39] Candidato Carnevale, G. (2019). Distributed model predictive control for power management in small-scale off-grid energy systems. <http://webthesis.biblio.polito.it/id/eprint/11350>

## **Abbreviations**

BESS	Battery energy storage system
MPPT	Maximum Power Point Tracker
PID	Proportional Integral Derivative
MPC	Model Predictive Controller
PV	Photovoltaic
GCPV	Grid-connected PV
ESS	Energy storage system
DG	Distributed generation
IC	Interlinking converter
DER	Distributed energy resources
AC-DC	Alternating current-direct current
RES	Renewable energy resources
MPCP	Model predictive current and power
MPVP	Model predictive voltage and power
FFT	Fast-Fourier Transform
THD	Total Harmonic Distortion
SoC	State of charge

PR	Performance ratio
STC	Standard Test Condition
KCL	Kirchoff's current law
Li-ion	Lithium-ion
Li-Po	Lithium polymer
Ni-MH	nickel-metal hydride